



Design of polyurea networks containing anticancer and anti-inflammatory drugs for dual drug delivery purposes

Mariane A. de Resende, Gabriele A. Pedroza, Lucia H. G. M. C. Macedo, Ricardo de Oliveira, Maria Amela-Cortes, Yann Molard, Eduardo F. Molina

► To cite this version:

Mariane A. de Resende, Gabriele A. Pedroza, Lucia H. G. M. C. Macedo, Ricardo de Oliveira, Maria Amela-Cortes, et al.. Design of polyurea networks containing anticancer and anti-inflammatory drugs for dual drug delivery purposes. *Journal of Applied Polymer Science*, 2022, 139 (16), pp.51970. 10.1002/app.51970 . hal-03512408

HAL Id: hal-03512408

<https://hal.science/hal-03512408>

Submitted on 28 Jan 2022

HAL is a multi-disciplinary open access archive for the deposit and dissemination of scientific research documents, whether they are published or not. The documents may come from teaching and research institutions in France or abroad, or from public or private research centers.

L'archive ouverte pluridisciplinaire **HAL**, est destinée au dépôt et à la diffusion de documents scientifiques de niveau recherche, publiés ou non, émanant des établissements d'enseignement et de recherche français ou étrangers, des laboratoires publics ou privés.

**Design of polyurea gel as versatile matrix bringing capabilities to carrier
separately and simultaneously anticancer and anti-inflammatory drugs for
delivery purposes**

*Mariane A. de Resende,¹ Gabriele A. Pedroza,¹ Lucia H. G. M. C. Macêdo,¹ Ricardo de Oliveira,¹
Maria Amela-Cortes,² Yann Molard,² Eduardo F. Molina^{*1}*

¹Universidade de Franca, Av. Dr. Armando Salles Oliveira 201, 14404-600 Franca, SP, Brazil

²Université Rennes, CNRS, ISCR - UMR 6226, ScanMAT – UMS 2001, F-35000 Rennes, France

Corresponding author: Eduardo F. Molina
*email: eduardo.molina@unifran.edu.br
ORCID : 0000-0002-3574-2923

Abstract

Naproxen (Nap), a non-steroidal anti-inflammatory drug, and 5-fluorouracil (5FU), an anticancer drug, were facile incorporated into a polyurea gel. Polyureas (PUr) were synthesized by one pot reaction via sol-gel chemistry. Soft segments were based on polyetheramine-PEO and hard segments were based on a hexamethylene diisocyanate trimer (HDI). The final materials were characterized by Fourier Transform Infrared Spectroscopy (FTIR), small-angle X-ray scattering (SAXS) and Differential Scanning Calorimetry (DSC). Polyurea can assume many forms revealing its versatility in terms of produced shapes. In good agreement with FTIR, SAXS studies showed a microphase separated structure arising from inter-hard-domain spacings which remains unchanged after incorporation of the drugs. DSC analysis demonstrated that the PEO chain mobility were poorly affected after the drugs incorporation due to the solvation of the drugs through the network. The water uptake and the amount of drug released agree well, playing an important role for controlled Nap and 5FU release. This work opens positive perspectives for ocular drug delivery and wound management, due to the easy processability of the gel, which has high feasibility to be moldable as pharmaceutical devices for contact lenses and transdermal patches purposes containing distinct therapeutic agents.

KEYWORDS: *sol-gel, poly(ethylene oxide), isocyanate crosslink, urea linkage, small-angle X-ray scattering, dual-drug release.*

1. Introduction

Nowadays, in the field of drug delivery devices, one of the main technological research forefronts is the development of functional materials able to load/release multi-drugs for combinatory therapy. Efficient treatments based on brand-new materials will overtake the place of traditional medical therapy for human health treatments. In this sense, drug delivery and controlled release by nanoparticles¹, nanovesicles², metal–organic frameworks (MOFs)³, liposomes⁴, microcapsules⁵, microporous materials⁶, clay minerals⁷, gel⁸ and hydrogels⁹ are highlighted areas, such as also systemic RNA delivery, drug delivery for localized therapy and oral/biological drug delivery systems.

A synergistic effect when combining drugs and administered together using a reservoir/carrier system has been widely observed.¹⁰⁻¹² In general, these drug combinations (dual-delivery) are applied for cancer therapy purposes.¹³ Harth's research group¹⁴ has developed several technologies for dual-drug delivery purposes.¹⁵⁻¹⁷ A dual drug formulation based on polyester nanosponge containing tamoxifen and quercetin showed potential therapeutic applications for both intravenous administration and oral delivery of drugs.¹⁶ In another work, Lockhart et al.¹⁵ demonstrated the feasibility of polyglycidol hydrogels as combinatory therapy for delivery of hydrophobic drugs and biological therapeutics. Moorthy *et. al*¹⁸ synthesized functional mesoporous organosilica hybrids as functional microcarriers for efficient incorporation of hydrophilic 5-fluorouracil (5FU) and hydrophobic ibuprofen (Ibu) drugs, showing a pH-triggered release of both drugs using a unique system.¹⁸

Functional materials originating from organic polymers (e.g., polyester, polyether, polycaprolactone, etc) could be used for world challenges depending on their chemical and morphological makeup. The simple production of polyurethane-polyureas presenting controlled and reproducible structure in a single processing step is a key advantage for developing novelty biomedical-health technologies. In particular, polyurea based materials that are obtained through the chemical reaction of polyisocyanates and a polyamine that create urea groups.^{19,20} The polyureas exhibit high resistance to pH changes, enhanced thermal stability with higher melting points and

1 better resistance to hydrolysis compared with polyurethanes.²¹⁻²³ These features are due to their
2 intrinsic ability to provide multiple donor-acceptor bonds, leading to novel arrangements of oxygen,
3 nitrogen and hydrogen atoms in urea groups²⁴ Polyurethanes and polyurea materials have been used
4 in biomedical applications^{25,26} due to their biocompatibility and excellent physical properties.²⁷
5
6

7
8 Considering the relevance of combining therapy and polymer systems for drug release
9 purposes, this work presents an elegant strategy for the simultaneous incorporation of two drugs with
10 distinct actions in a unique polymeric material. The concept described is utterly simple; that is, once
11 loaded, both drugs are preserved in the polyurea network and released in water. As far as we know,
12 there are still no reports on the use of polyurea gel (based on Jeffamine-PEO and isocyanate
13 crosslinker) as a versatile approach for dual-drug delivery purposes. A simple reaction between an
14 amino-terminated-polyether PEO (Jeffamine ED-2003) and a tridentate ligand hexamethylene
15 diisocyanate trimer (HDI) at room temperature led to the formation of a transparent, flexible, and
16 scalable polymeric device for medical purposes. The presence of functional groups (urea, oxygen
17 ether-type) and a long polymer chain extent of the polyurea allowed remarkable dissolution
18 (separately or simultaneously) of the anticancer therapeutic agent 5-fluorouracil and the non-steroidal
19 anti-inflammatory naproxen drug.
20
21
22
23
24
25
26
27
28
29
30
31
32
33
34
35
36
37

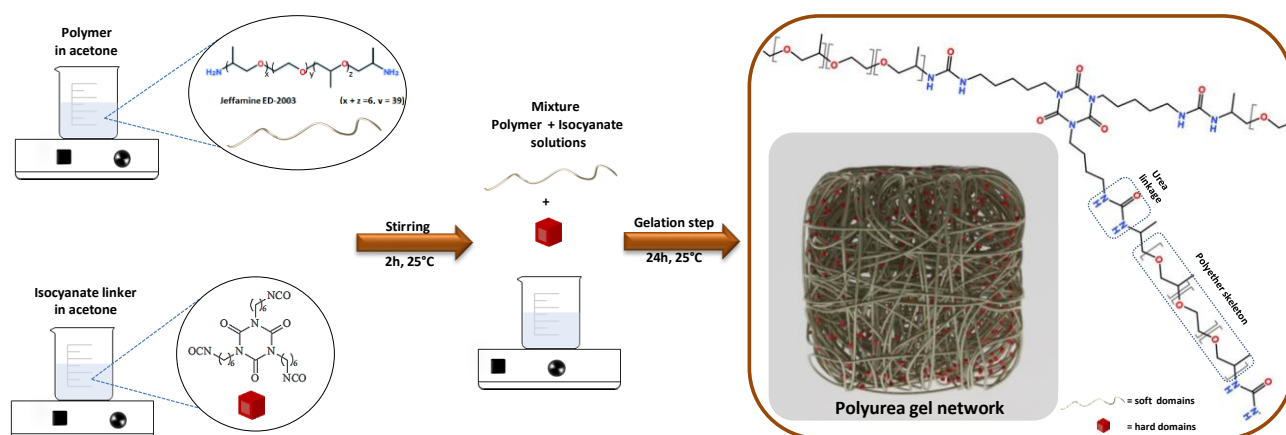
38 **2. Experimental Section**

40 **2.1 Materials**

41
42 Naproxen (Nap), 5-Fluorouracil (5FU) and acetone were purchased from Sigma-Aldrich.
43
44 O,O'-bis-(2-aminopropyl)polypropylene glycol-block-polyethylene glycol-block-polypropylene
45 (Jeffamine ED2003 - PEO block with a molecular weight of 1900 g mol⁻¹) was donated by Huntsman
46 Performance Products (Brazil). The crosslink hexamethylene diisocyanate trimer-HDI (Desmodur
47 N3300 with a molecular weight of ~ 504 g mol⁻¹) was provided by Bayer Corporation. All reagents
48 were used without further purification.
49
50
51
52
53
54
55
56
57
58
59
60
61
62
63
64
65

2.2 Synthesis of polyurea gels

The polyurea gel was obtained through the sol-gel process as previously demonstrated in literature.^{28,29} To obtain the polyurea gel, tridentate ligand HDI was covalently bonded to the PEO (Jeffamine ED-2003) by reaction of the isocyanate groups and the primary amino groups attached to the end of the polyether backbone of PEO. In brief, the PEO macromonomer (4g, 2.10×10^{-3} mol) and the HDI cross-linker (1g, 1.98×10^{-3} mol) are first dissolved in separated beakers using acetone, at room temperature ($\sim 25^\circ\text{C}$), to form homogenous solutions. The molar ratio of PEO:HDI used was 1:0.94. The HDI solution was slowly added dropwise to the PEO solution, while stirring at room temperature, until completely dissolved. The resulting solution was poured into Teflon molds and then kept at 25°C for 24 h for gelation. After the PEO:HDI reaction, the hard domains (isocyanurate rings) are connected and randomly disperse through the polymer chains by urea linkage (**Scheme 1**).



SCHEME 1

2.3 Synthesis of polyurea gels containing drugs

Samples containing drug (Nap, 5-FU or both drugs) were prepared *via* one-step sol-gel process. The drug concentration of 1 wt% (with respect to the mass of PEO) was dissolved in acetone and then mixed with PEO to obtain a homogeneous solution. The HDI solution was dissolved in separated beaker and added as cited above to form the loaded polyurea samples. The resulting mixture was poured into Teflon mold and gelled using the same conditions (temperature and time) than the

ones used for the pure polyurea. The drug content was embedded into the polyurea network during the gelation process. The final materials were named PUr (polyurea gel), PUr-Nap (polyurea containing 1 wt % of Nap), PUr-5FU (polyurea containing 1 wt % of 5FU) and PUr-Nap-5FU (polyurea containing 1 wt % of both drugs incorporated simultaneously).

2.4 Characterization

The structural characterization of PUr gels was performed by Transform Infrared Spectroscopy (FTIR) and small-angle X-ray scattering (SAXS). FTIR spectra was recorded at 3100-700 cm^{-1} by ATR mode using a Perkin Elmer Frontier spectrometer, with a resolution of 2 cm^{-1} and average of 32 scans. Small angle X-ray scattering (SAXS) experiments were conducted using a Nano-InXider (Xenocs). X-rays of wavelength $\lambda = 1.54 \text{ \AA}$ was used, and the measurements was performed at sample-to-detector distance of 938 mm to cover a q -range of $0.009 < q < 0.45 \text{ \AA}^{-1}$, where $q = (4\pi/\lambda) \sin (\theta/2)$ corresponding the magnitude of the scattering vector, and θ is the scattering angle. All the measurements were recorded at room temperature ($\sim 25^\circ\text{C}$). The thermal features of the polyurea (loaded and unloaded) was studied by Differential Scanning Calorimetry (DSC) on a TA25 DSC. Disk sections of approximately 10 mg were cut off from the organogels and placed in 40- μL aluminium containers. Each sample was heated from -80 to 250°C at a rate of $10^\circ\text{C min}^{-1}$ using argon as the purge gas.

2.5 Water uptake features

The contact angle of the polyurea matrix was measured using an OCA (Dataphysics) contact angle instrument in sessile drop mode. The droplet volume used was about 7.0 μL of deionized water, followed by a liquid droplet that was delivered onto the polyurea surface. Contact angle values and images were obtained using the drop shape analysis software, which is described by the Young-Dupré equation, assuming a smooth and homogeneous surface.³⁰

The swelling behavior of the unloaded and loaded PUr samples were studied using a

gravimetric method. The gel samples (~ 0.5 g and 2mm thickness) were immersed in distilled water kept at 25 °C. The swollen samples were removed from the water at the predetermined time, gently dried between two filter papers to remove any excess water on the surface, and weighed in an electronic analytical balance (Ohaus, PA214CP model). The swelling ratio (S) was determined using the equation:

$$S = \frac{Ws - Wd}{Wd} * 100$$

where Ws and Wd are the mass of swollen and dry samples, respectively.

2.6 *In vitro* drug release assays

Temporal release of Nap and 5FU separately and, release simultaneously was evaluated in distilled water (100 mL, pH 6) using ~0.5 g of PUr containing individual or both drugs loaded. The release assays were carried out at a controlled temperature of 37 °C, under constant stirring (100 rpm). The *in vitro* studies were performed by UV-Vis spectroscopy, using a Cary60 dual-beam spectrophotometer (Agilent Technologies) connected to an immersion probe (optical path length of 2 mm). Quantitative determination of the cumulative 5-FU and Nap released were performed using a calibration curve constructed using the maximum absorbance values at $\lambda_{\max}=229$ nm (Nap) and $\lambda_{\max}=265$ nm (5FU) of drugs solutions at different concentrations (**Figures S1a-b**). All release assays were performed with two independent samples and the results are presented as data averages.

3. Results and Discussion

3.1 *Structural properties*

The formation of PUr gel (presence of –NH– from urea) and possible interactions between drugs and PUr were analyzed by FTIR. **Figure 1** shows the FTIR spectrum of PUr unloaded and loaded with Nap, 5FU and both drugs simultaneously. The full spectra collection of FTIR data from 700-3000 cm^{-1} is presented in **Figure 1a**. The presence of isocyanate groups are considerably toxic and moisture sensitive, thus isocyanate free polyureas is now attracting research interest due to its

potential application in different areas such as optics, environment and health. The isocyanate HDI crosslink presents an intense band at 2266 cm^{-1} characteristic of $\text{N}=\text{C}=\text{O}$ asymmetric stretching as reported in the literature.²⁹ The PUr gel (**Figure 1 black line**), show the absence of the $\text{N}=\text{C}=\text{O}$ band revealing that the matrix is isocyanate-free using the synthesis procedure. Furthermore, no remanescant isocyanate groups were observed for loaded PUr matrices (**Figure 1 red, blue and green lines**) demonstrating great potential for health application using this class of polyurea obtained by simple PEO (Jeffamine) and HDI reaction. A close inspection of the FTIR spectrum of unloaded and loaded PUr in the region between $1300\text{--}1750\text{ cm}^{-1}$ (**Figure 1b**) and $700\text{--}1300\text{ cm}^{-1}$ (**Figure 1c**) showed bands assigned to the $\text{C}=\text{O}$ stretching (urea linkage) and others associated to ethylene rocking vibrations ($\nu(\text{CH}_2)$), $(\text{C}-\text{O}-\text{C})$ stretching vibrations ($\nu(\text{COC})$) of the polyether PEO backbone.³¹ The bands originated from urea groups in the region between 1500 and 1800 cm^{-1} (**Figure 1b**) correspond to the “amide I” and “amide II” vibrational modes, assigned to $\text{C}=\text{O}$ stretching, $\text{C}-\text{N}$ stretching, $\text{C}-\text{C}-\text{N}$ deformation vibrations, $\text{N}-\text{H}$ in-plane bending, and $\text{C}-\text{C}$ stretching. The shoulder at 1719 cm^{-1} was attributed to free $\text{C}=\text{O}$ groups and the 1688 and 1643 cm^{-1} corresponded to H-bonds in a more ordered domain.³² The region between 700 and 1300 cm^{-1} (**Figure 1c**) is characteristic of the polymer backbone, which is very sensitive to conformational changes of the PEO chains. The very intense band at 1102 cm^{-1} was attributed to $\text{C}-\text{O}$ stretching absorption and the vibrations of the $\text{C}-\text{C}$ stretching was found at 950 , 1037 and 1247 cm^{-1} . Incorporation of the individual drugs (**Figure 1, red and blue lines**) and Nap and 5FU simultaneously (**Figure 1, green line**) into PUr did not affect the structure of the gel, showing similarities between the FTIR spectra of unloaded and loaded PUr. This indicates a notable solvation of Nap and 5FU drugs (individual or simultaneously) by the PUr matrix and confirms that both structures (matrix and drug) are preserved after incorporation of drugs into the polyurea network. Regardless of the presence or not of drugs into PUr gel, transparent and rubbery samples were obtained (**Figure S2**). Furthermore, versatile shaping of fabricated samples were demonstrated (**Figure 2**) due to the easy processability of the gel, which had high feasibility to be moldable as pharmaceutical devices for contact lenses and transdermal patches purposes.

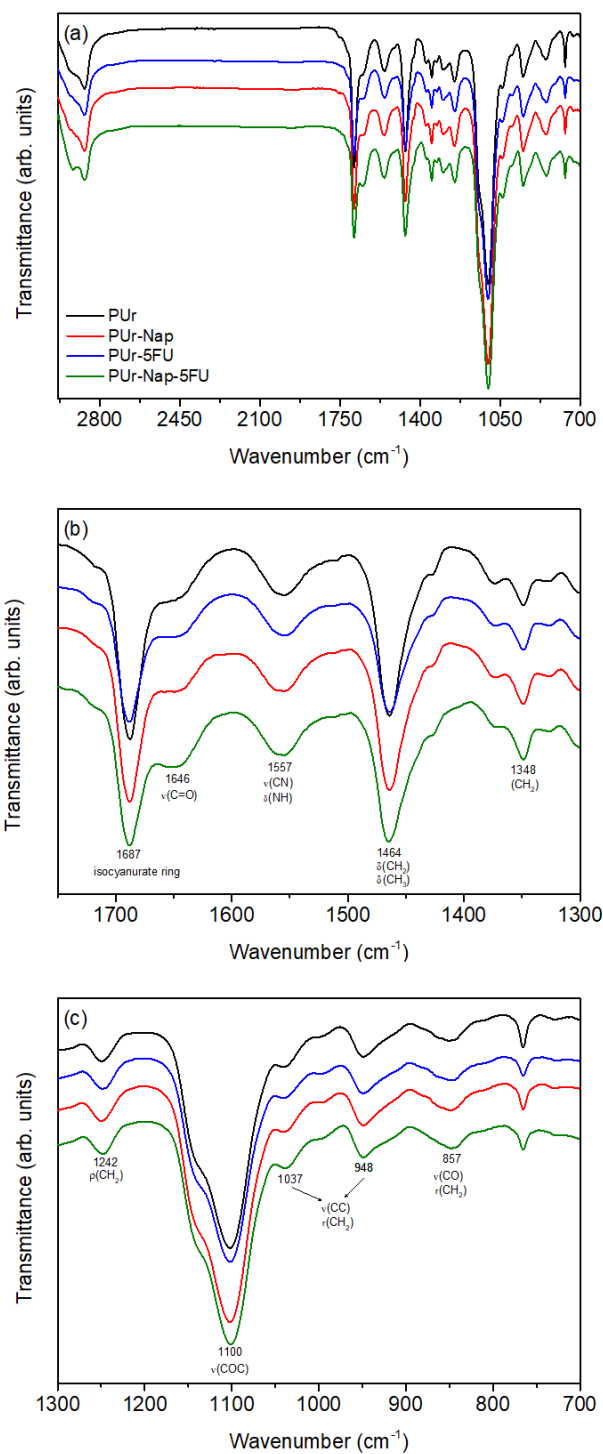


FIGURE 1

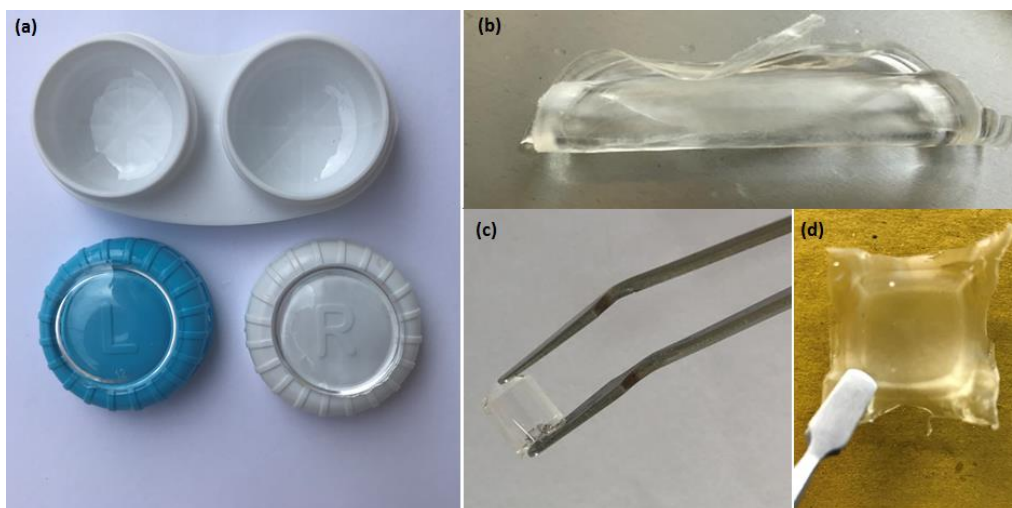


FIGURE 2

Microphase separation behavior of PUr samples was investigated by small angle X-ray scattering SAXS (**Figure 3, panel a**). The SAXS curve of unloaded PUr displays a single broad peak with maxima centered at $q_{\text{max}} = 1.13 \text{ nm}^{-1}$, reflecting the microphase separation at ambient temperature. This correlation peak evidences a spatial correlation between the hard domains randomly dispersed in the polymer matrix (represented in **Figure 3 panel b**). The position of the interference peak was used to estimate the d spacing ($d = 2\pi/q_{\text{max}}$), which is characteristic as an average interdomain spacing arising from the presence of periodic structure^{33,34} (on a short-range scale length). The mean inter-hard-domain spacings, $d \sim 56 \text{ \AA}$, calculated by $2\pi/q_{\text{max}}$ (**Figure 3 panel b**) and the shapes of the SAXS profile for the polyurea containing drugs (separately or simultaneously) were similar. This demonstrates that the microstructure of PUr gel is not affected by the incorporation of Nap/5FU. However, we noticed a decrease in the intensity of the correlation peak for polyurea samples containing Nap or 5FU (separately) compared with unloaded PUr. These features suggest that the correlation peak resulting from the interdomain spacing was masked by additional scattering of the drug. The SAXS curve for polyurea sample containing both drugs confirms that the microphase structure of PUr remains unchanged, which a similar SAXS curve shape was showed. These findings agree well with FTIR results, and swelling/release assays discussed below.

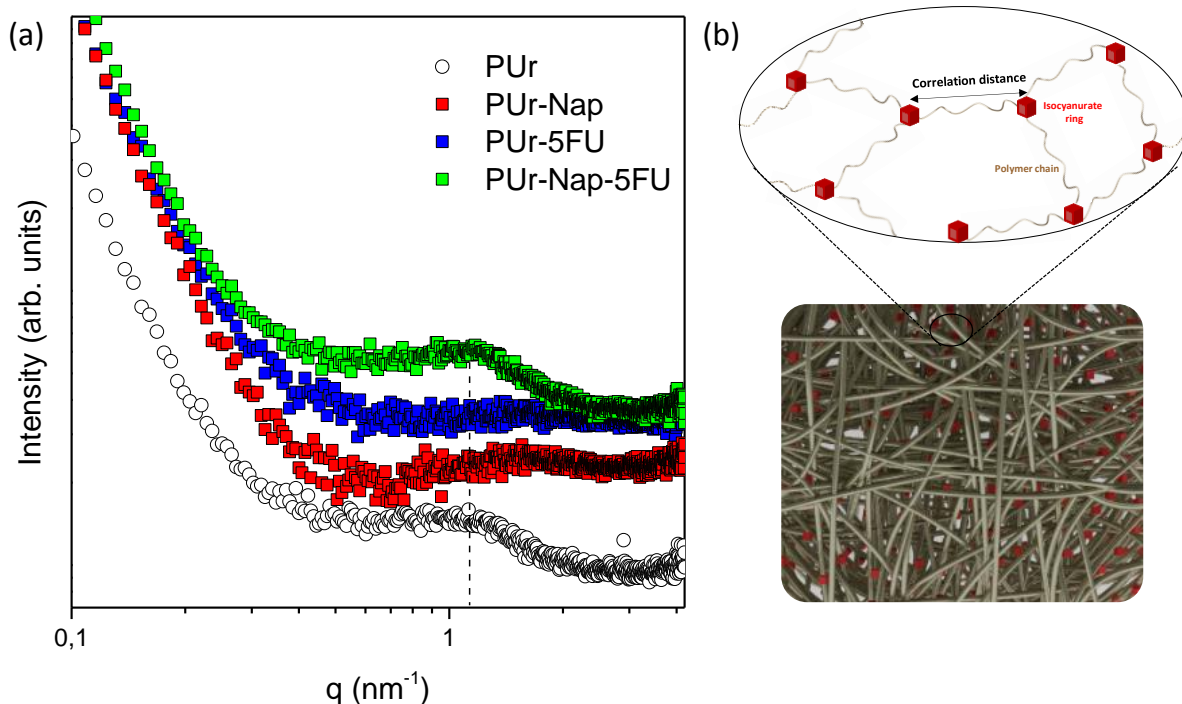


FIGURE 3

3.2 Swelling behavior

Figure 4 shows the surface wettability and contact angle images (inset of Figure 4) of PUr as a function of time. The initial value of θ for PUr after contact with the water droplet was $80 \pm 0.4^\circ$. This value indicates that PUr is wettable due to the hydrophilic nature of i) PEO chains and ii) the existence of urea groups in the gel. As expected, the θ value decreases as a function of time, from the initial $80 \pm 0.4^\circ$ (at 0 min) to $45 \pm 0.4^\circ$ (after 5 min in contact with the water droplet). This behavior indicates good wetting of PUr by water. The fast wettability of the gel can play an important role on the release profile of species in water for drug delivery purposes.

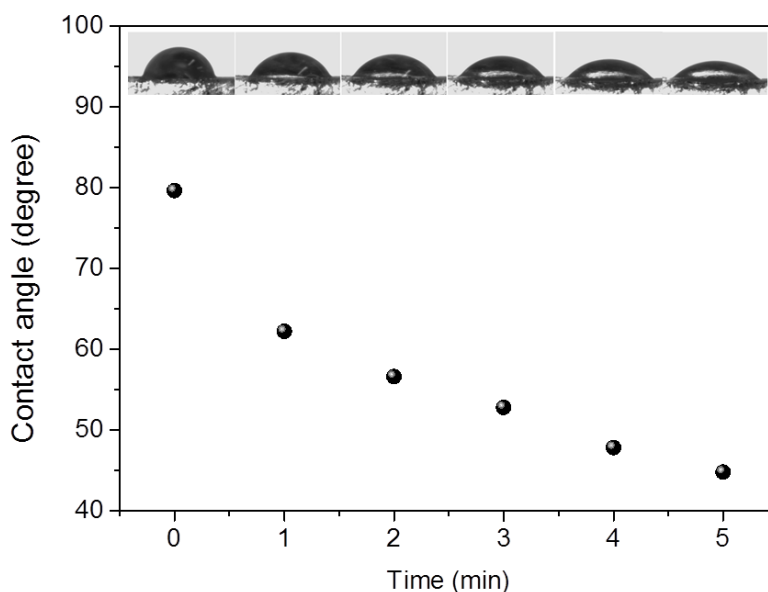


FIGURE 4

Figure 5 represents the evolution of swelling capacity as a function of time of the unloaded and drug loaded PUr. Due to the hydrophilic nature of PEO, a swelling capacity of ~230% for PUr sample was observed at final assay ($t = 300$ min) (**Figure 5- black symbols**). This feature can be attributed to the hydration (water uptake) of the PUr matrix, which induces the expansion of the network. Similar swelling capacity was obtained for the polyurea PUr-5FU (**Figure 5 - green symbols**), while in the case of PUr-Nap, a swelling capacity of 300% was achieved with 300 min of assay (**Figure 5 – blue symbols**), respectively. The swelling profile of PUr is different from the ones of PUr-Nap and PUr-5FU during the first 60 min of assays. A decrease of water uptake from 220% (PUr) to 161 and 135% (PUr-Nap and PUr-5FU, respectively) at the initial stage of hydration ($t = 60$ min) is observed and can be attributed to the presence of drugs through the polyurea network. A hinder effect of hydration indicates a barrier in water flux through the polymer chains due to the presence of both drugs simultaneously into PUr matrix (**Figure 5 – pink symbols**). Such behaviors will be discussed below and correlated to release assays.

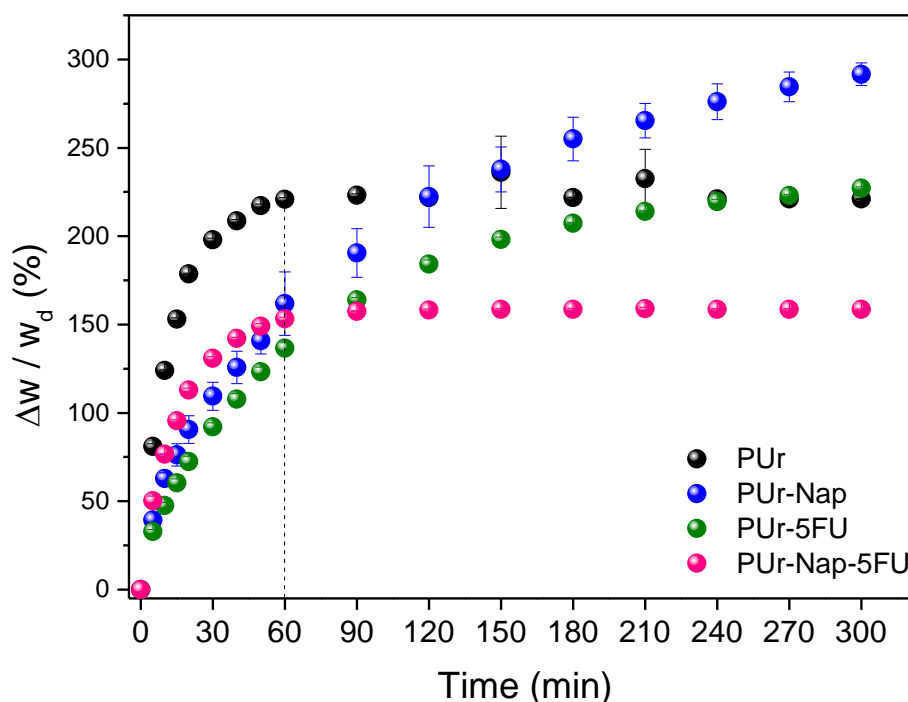


FIGURE 5

3.3 Thermal behavior

Differential scanning calorimetry (DSC) measurements were performed to study the chain mobilities of the PUr materials. In general, Jeffamine-PEO based materials exhibit low glass transition (T_g), and a first order reversible thermal transformation characteristic of crystallization-melting (T_m) of the PEO ethylene moities.^{35,36} Independently of the PUr (unloaded and loaded with drugs) these two events (T_g and T_m) were observed in the DSC thermograms, characterizing the semicrystalline PEO with a molecular weight of 1900 g mol⁻¹ (**Figure 5**). The unloaded PUr shows a T_g at approximately -59 °C, characteristic of the difference between the heat capacities of the glass and rubber states. The melting of the PEO crystalline phase appears as an endothermic peak at around 28°C (**Figure 5 black line**), allowing to calculate the crystallinity degree (D_C) of the samples, as follows:

$$D_C = \frac{\Delta H_m}{\Delta H_m^0} \times 100\% \quad (1)$$

where ΔH_m is the melting enthalpy per gram of PEO in the PUr organogel, and ΔH_m^0 is the

melting enthalpy for 100% crystalline PEO (188.9 J/g).³⁷

Table 1 provides the values of the thermal properties (T_g , T_m and D_c) obtained from DSC analyses (**Figure 5**). A decrease in the crystallinity degree (D_c) was observed for the loaded PUr samples with Nap, 5FU and both drugs simultaneously, in comparison with PUr. The D_c decrease is followed by a change in the melting temperature (T_m) of the polyether-PEO, suggesting a perturbation in the dynamics of the PEO chains in the molten state.³⁸ These findings indicate that the drugs were loaded (separately or simultaneously) into polyurea matrix presenting weak interactions with the functional groups of the PUr matrix such as ether-type oxygen atoms (from polyether skeleton) and urea, in agreement with the FTIR results (**Figure 1**). The slight T_g changes (**Table 1**) from -59 (PUr pure) to -58°C (PUr-Nap), -54°C (PUr-5FU) and -56°C (PUr-Nap-5-FU) corroborate the conclusion that the PEO chain mobility and inter-chain interactions were poorly affected after the drugs incorporation.

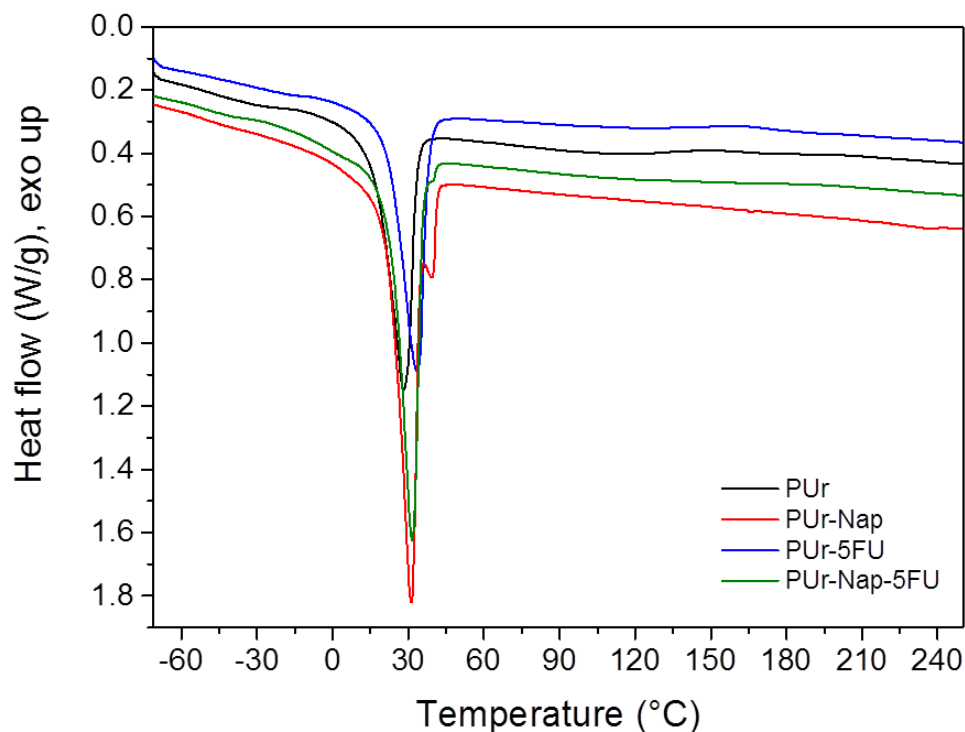


FIGURE 6

3.3 Drug release studies

Figure 7 shows the UV-vis spectra and cumulative profiles in the aqueous medium for individual and dual-drug release from the PUr samples loaded with Nap and 5FU. The amount (%) of drug released from PUr was determined from *in situ* monitoring of the maximum absorbance of the drug molecules ($\lambda_{\text{max}} = 229 \text{ nm}$ and 265 nm for Nap and 5FU, respectively). Irrespective of the drug loaded into the PUr gel, UV-vis data collected during the release experiments demonstrated an increase of the band corresponding to Nap and 5FU, indicating that the drug concentration increases as a function of time (see **Figure 7a and 7c**). The dual release concept is clearly noted by the time evolution of both UV-vis bands in the spectral data of **Figure 7e**. The presence and increase of Nap and 5FU bands (simultaneously) show high potential of the PUr gel as a functional carrier to incorporate different species in a one-step synthesis route.

The cumulative release profiles of the individual drugs from the loaded PUr with Nap and 5FU are displayed in **Figures 7b and 7d**, respectively. The dissolution and release of drugs by PUr was facilitated due to the gel wettability (see **Figure 4** contact angle measurements) and the hydrophilic nature of PEO chains.^{39,40} The cumulative release amounts of Nap and 5FU (individual) were 80% and 60% in the first 150 min and then reached a near equilibrium-state (**Figures 7b and 7d**). The final amount of each individual drug released by PUr was different at the assays' end. Opposite results were expected since 5FU has a hydrophilic nature, while Nap has major hydrophobicity. The use of ureasil-PEO hybrids as carriers for dual-drug release purposes was already reported previously.⁴¹ The amount of Nap and 5FU released is quite different to those previously found for the di-ureasils hybrids. In the present work, the high Nap amount released could be attributed to i) the weak interactions between Nap and the host matrix (see **Figure 1 FTIR results**), and ii) the exposed drug on the PUr surface leading to a dissolution of the Nap in the aqueous medium. The water uptake and the Nap release profiles monitored by gravimetric method and UV-vis, respectively, can be explained as follows. When the Nap-loaded PUr matrix is immersed in water, the drug molecules located close to the host surface begin to dissolve followed by a deceleration in

swelling ratio. Due to the Nap hydrophobic nature, this drug could act as a barrier hindering the diffusion of water molecules inside the matrix. This feature leads to a water uptake decrease, compared to the unloaded PUr matrix during the initial (60 min) swelling assays (see **Figure 5**). The most dissolved solute (Nap drug) extracted from the surface of PUr was observed at 150 min (80% released). From this time, a water flux arises into the polyurea matrix, which in turn, accelerates the hydration and expansion of the network free volume reaching a swelling capacity of 300%, as observed in **Figure 5** (blue symbols). During the first 150 min of immersion into water, a good agreement between the swelling and release profile of PUr-Nap is observed (**Figure S3**). This finding clearly points out the contribution of the drug in hindering the hydration, and, at an advanced stage ($t > 150$ min and amount of Nap release $> 80\%$), the water flow continues, favouring the network expansion and consequently the diffusion of drug.

It can be seen that about 72% of 5-FU was released from PUr within 360 min (**Figure 7d**). The PUr matrix was able to release 5FU in a bimodal pattern, characterized by a faster release followed by a sustainable release. The initial burst release (68% , $t = 180$ min) can be due to the diffusion and weakly bonded 5FU molecules located on the polyurea surface. Moreover, the presence of 5FU into the polyurea network also evidences the influence of the drug in the water uptake behavior (**Figure 5**). The dissolution/diffusion of 5FU in the bulk is hampered by the surface 5FU molecules in the PUr gel. This suggested that the 5FU onto the external surface of polyurea is easily and quickly diffuse to the aqueous solution. The release of 5FU located deeply inside the network (bulk) can be hindered probably due to inter- and intramolecular interactions between the drug and ether-type oxygen atoms of the polyether phase. These results agree well with the observed thermal properties: PUr-5FU sample shows a major glass transition (T_g) change and melting temperature (T_m) increase compared to PUr-Nap (see **Table 1**).

The curve profiles for dual-release of NAP/5FU from PUr are shown in **Figure 7f**. The release behavior seems to be similar compared to the individual drug release curves (**Figures 7b and 7d**). However, the amount of drugs simultaneously released compared with the individual profiles within

150 min of assay were lower, ~ 60% (Nap released) and ~ 40% (5FU released), respectively. These features are in good agreement with hydration (swelling properties) of the PUr-Nap-5FU sample, which the presence of both drugs hinders the water molecules diffusion through the polymeric chains hence decrease the amount release compared with separately profiles in the same time $t = 150$ min (see details in **Table S1**).

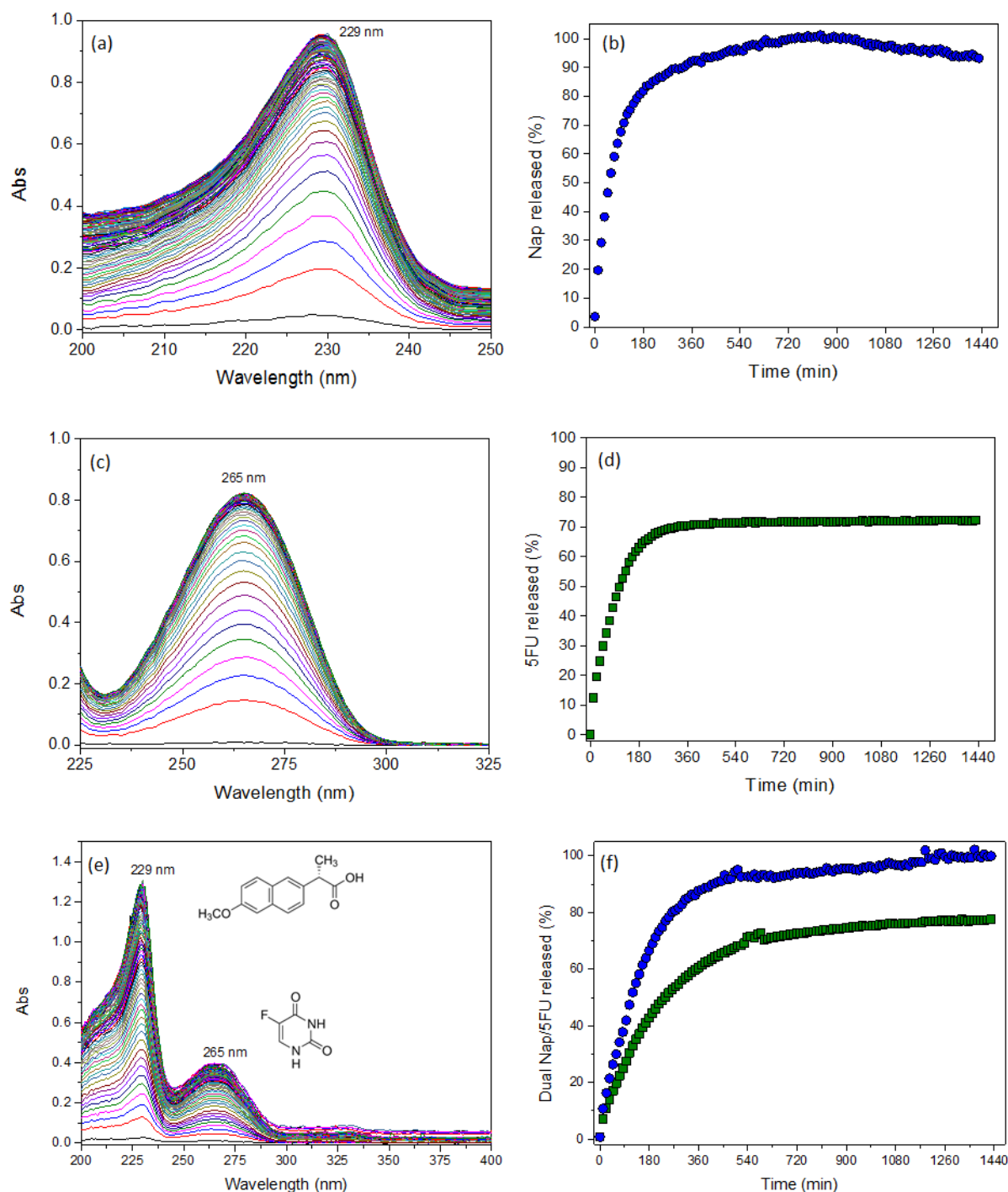


FIGURE 7

The Korsmeyer-Peppas model⁴² (see details and equation - **Supporting information**) was used to determine the transport mechanism of the individual- and dual-release of Nap and 5FU from the PUr gel. The release mechanism is characterized by the exponent n . Fickian diffusion is indicated by n value of 0.50, Case II transport indicate zero-order drug release with n value of 1, while an anomalous transport mechanism is indicated by an n value of 0.50 – 1.0.

The release curves, plotted as $\log (M_t/M_\infty)$ vs. $\log t$, of individual and dual-release of Nap and 5FU from the PUr gel are shown in **Figure 8**. The kinect curves of all loaded PUr samples with Nap and 5FU (individually and simultaneously) were fitted with one straigh line. The experimental n value obtained for individual Nap and 5FU release (**Figure 8a,b**) was $n = 0.62$. This n value indicates an anomalous transport attributed to the diffusion/zero-order rate of drug controlled by the penetration of the water-swollen front. In the case of simultaneous drug release (**Figure 8c**), n values of 0.68 (5FU) and 0.70 (Nap) were observed, showing the same mechanism as individual profiles. The coefficient of determination (R^2) for all samples was 0.99, indicating that the release of 5FU/Nap was well fitted with the Korsmeyer-Peppas model (see details in **Table S1**). The lower amount of drugs released simultaneously compared with the individual systems in the same period of time (150 min) suggests that the presence of both drugs (Nap + 5FU) on the surface and depth (bulk) within the gel causes a hindered effect suggesting (i) a hydrophilic/hydrophobic balance created by the loaded drugs into PUr network, and (ii) weak interactions between polymer-drug.

This work presents, for the first time, a drug pair (naproxen Nap, and 5-fluorouracil 5FU) could be facile embedding into a polyurea gel by one step process at mild temperature. Moreover, this class of polyurea could be used to control the Nap and 5FU release separately, and release Nap/5FU simultaneously. Due to the physical-chemical properties, biocompatibility²⁹ and stability of the gels, these materials could be fabricated as contact lenses, films and LED shapes open up positive perspectives to prepare multifunctional materials for health, optical, and environmental applications.

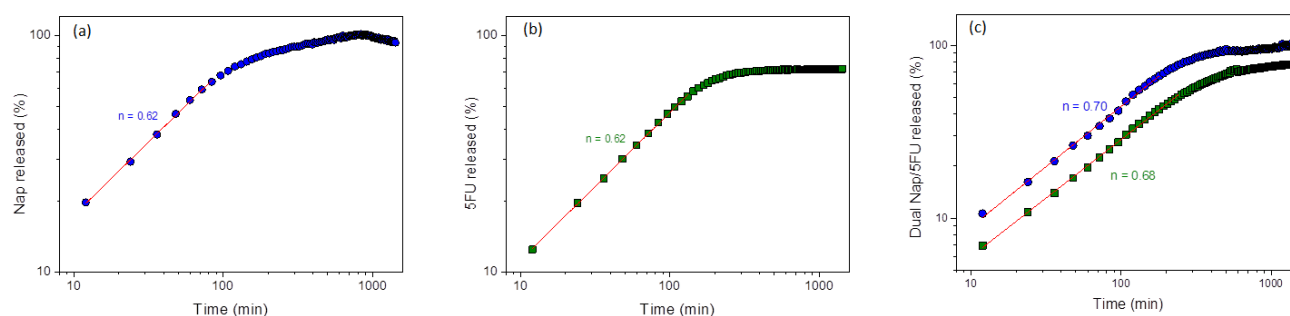


FIGURE 8

4. Conclusions

In the present work, the possibility to easily incorporate two drugs simultaneously into a polyurea gel by one-step sol-gel chemistry was demonstrated. Moreover, due to the polyether long chain and the urea groups formed in the matrix, it was possible to dissolve an anti-inflammatory (Naproxen) and an anticancer (5-fluorouracil) drug with distinct hydrophilicity in the PUr gel. The presence of urea groups and free isocyanate of the final materials was confirmed by FTIR. Besides, no changes detected by FTIR spectra of unloaded and loaded PUr evidences great drug dissolution (1 wt %) through the gel, suggesting weak interactions between the drugs and the host matrix.

The PUr material showed fast surface wettability that led to a contact angle decrease from 80 to 45° after the first initial minutes in contact with the water droplet. Thermal features (DSC analysis) revealed a rigidity increase (glass transition T_g) of the polymer chains with the PUr containing 5FU (individually or together with Nap) and changes in the crystallinity degree (D_c) of the loaded drug samples. The successful dual-drug release highlights the polyurea gel as a versatile carrier to combine anti-inflammatory and anticancer drugs into a single polymer matrix, opening new opportunities to develop functional materials containing different species for optical, health and environmental applications. Thus, the strategy to use polyurea material to design multicomponent drug@PUr is quite promising for simultaneous delivery of 5-FU and Nap to achieve synergistic anticancer effects.

Acknowledgements

This work was supported by the Coordenação de Aperfeiçoamento de Pessoal de Nível Superior CAPES – Finance Code 001, Conselho Nacional de Desenvolvimento Científico e Tecnológico CNPq – n° 306271/2017-6, and Fundação de Amparo à Pesquisa do Estado de São Paulo FAPESP grant 2019/17860-9, 2020/06531-1, FAPESP SPRINT grant 2017/50286-9 and CNRS (PRC Clustobrane) The authors are grateful to Celso V. Santilli and Rodrigo Santos for SAXS measurements. We thank Huntsman Performance Products and Bayer Group for donating the Jeffamine® and triisocyanate crosslinker reagents, respectively.

Supporting Information: Figure S1 analytical curves of naproxen and 5-fluorouracil drugs, Figure S2 photograph of the unloaded and loaded polyurea samples, Figure S3 comparison between profile release and water uptake behavior for PUr-Nap sample. Korsmeyer–Peppas equation and Kinect parameters, Table S1 showed the amount released of the drugs at different times, mechanism of release (n), and coefficient of determination (R^2)

Author Contributions: All the authors planned and discussed the results. The manuscript was written through contributions of all authors. All authors have given approval to the final version of the manuscript.

There are no conflicts of interest to declare.

References

1. M. Kundu, P. Sadhukhan, N. Ghosh, S. Ghosh, S. Chatterjee, J. Das, G. Brahmachari, P. C. Sil, *Mater. Sci. Eng. C* **2021**, *126*, 112142.
2. Kanchanapally, R.; Deshmukh, S. K.; Chavva, S. R.; Tyagi, N.; Srivastava, S. K.; Patel, G. K.; Singh, A. P.; Singh, S. *Int. J. Nanomed.* **2019**, *14*, 531– 541.
3. Shi, L.; Wu, j.; Qiao, X.; Ha, Y.; Li, Y.; Peng, C.; Wu, R. *ACS Biomater. Sci. & Eng.* **2020**, *6*, 4595-4603.
4. Lai, W.; Wong, W.; Rogach, A. L. *ACS Appl. Mater. Interfaces* **2020**, *12*, 43341-43351.
5. Huang, G.; Zhang, Z.; Cheng, L.; Xiao, J. *Mater. Sci. Eng. C* **2019**, *105*, 110129.
6. Wang, J.; Zhou, J.; Xu, D.; Li, J.; Deng, D. *ACS Appl. Mater. Interfaces* **2020**, *12*, 47197–47207
7. Sharifzadeh, G.; Hezaveh, H.; Muhamad, I. I.; Hashim, S.; Khairuddin, N. *Mater. Sci. Eng. C* **2020**, *110*, 110609.

8. Ramin, M. A.; Sindhu, K. R.; Appavoo, A.; Oumzil, K.; Grinstaff, M. W.; Chassande, O.; Barthélémy, P. *Adv. Mater.* **2017**, *29*, 1605227
9. Türk, S.; Altınsoy, I.; Efe, G. Ç.; Ipek, M.; Özacar, M.; Bindal, C. *Mater. Sci. Eng. C* **2021**, *121*, 111829.
10. Lehar, J.; Krueger, A. S.; Avery, W.; Heilbut, A. M.; Johansen, L. M.; Price, E. R.; Rickles, R. J.; Short, G. F.; Staunton, J. E.; Jin, X. W.; Lee, M. S.; Zimmermann, G. R.; Borisov, A. A. *Nat. Biotechnol.* **2009**, *27*(9), 864-864.
11. Xu, M.; Xu, C. X.; Bi, W. Z.; Song, Z. G.; Jia, J. P.; Chai, W.; Zhang, L. H.; Wang, Y. *Bone* **2013**, *57*(1), 111-115.
12. Scarano, W.; de Souza, P.; Stenzel, M. H. *Biomater. Sci.* **2015**, *3*(1), 163-174.
13. Xu, M.; Xu, C. X.; Bi, W. Z.; Song, Z. G.; Jia, J. P.; Chai, W.; Zhang, L. H.; Wang, Y. *Bone* **2013**, *57*, 111-115.
14. <https://www.harth-research-group.org/>
15. Lockhart, J. N.; Beezer, D. B.; Stevens, D. M.; Spears, B. R.; Harth, E. *J. Control. Rel.* **2016**, *244*, 366-374.
16. Lockhart, J. N.; Stevens, D. M.; Beezer, D. B.; Kravitz, A.; Harth, E. *J. Control. Rel.* **2015**, *220*, 751-757
17. Gilmore, K. A.; Lampley, M. W.; Boyer, C.; Harth, E. *Adv Drug Deliv Rev.* **2016**, *98*, 77-85.
18. Moorthy, M. S.; Bae, J.; Kim, M.; Kim, S.; Ha, C. *Part. Part. Syst. Charact.* **2013**, *30*, 1044-1055
19. Stanford, J. L.; Still, R. H.; Wilkinson, A. N. *Polym. Int.* **1996**, *41*, 3, 283-292.
20. Fragiadakis, D.; Gamache, R.; Bogoslovov, R.; Roland, C. *Polymer* **2010**, *51*, 1, 178-184.
21. Roland, C.; Twigg, J.; Vu, Y.; Mott, P. *Polymer* **2007**, *48*, 2, 574-578.
22. Mariappan, T.; Wilkie, C. A. *Polymer* **2013**, *58*, 5, 371-384.
23. Cao, H.; Li, B.; Jiang, X.; Zhu, X.; Kong, X. Z. *Chem. Eng. J.* **2020**, *399*, 1, 125867.
24. Tuerp, D.; Bruchmann, B. *Macromol. Rapid Commun.* **2015**, *36*, 2, 138-150.
25. Shaikh, M.; Choudhury, N. R.; Knott, R.; Kanwar, J. R.; Garg, S. *Eur. J. Pharm. Biopharm.* **2016**, *101*, 82-89.
26. Cass, P.; Knowler, W.; Hinton, T.; Shi, S.; Grusche, F.; Tizard, M.; Gunatillake, P. *Acta Biomater.* **2013**, *9*, 8299-8307.
27. Hergenrother, R. W.; Yut, X. H.; Cooper, S. L. *Biomater.* **1994**, *15*, 635-640.
28. Sanchez-Ferrer, A.; Rogez, D.; Martinoty, P. *Macromol. Chem. Phys.* **2010**, *211*, 1712-1721.
29. Bonattini, V. H.; Paula, L. A. L.; de Jesus, N. A. M.; Tavares, D. C.; Nicolella, H. D.; Magalhães, L. G.; Molina, E. F. *Polym Int.* **2020**, *69*, 5, 476-484.
30. Howe, J. *Int. Mater. Rev.* **1993**, *38*, 233-256.

31. Molina, E. F.; Pulcinelli, S. H.; Santilli, C. V.; Blanchandin, S.; Briois, V. *J. Phys. Chem. B* **2010**, *114*, 3461–3466.
32. Carlos, L. D.; Bermudez, V. Z.; Amaral, V. S.; Nunes, S. C.; Silva, N. J. O.; Sa Ferreira R. A.; Rocha, J.; Santilli, C. V.; Ostrovskii, D. *Adv. Mater.* **2007**, *19*, 341–348.
33. Jesus, N. A. M.; Oliveira, R.; Amela-Cortes, M.; Dumait, N.; Cordier, S.; Molard, Y.; Molina, E. F. *Dalton Trans.* **2021**, 50, 8907.
34. Feula, A.; Tang, X.; Giannakopoulos, I.; Chippindale, A. M.; Hamley, I. W.; Greco, F.; Buckley, C. P.; Siviour, C. R.; Hayes, W. *Chem. Sci.* **2016**, *7*, 4291–4300.
35. Molina, E. F.; Pulcinelli, S. H.; Briois, V.; Santilli, C. V. *Polym. Chem.* **2014**, *5*, 1897–1904.
36. Molina, E. F.; Jesus, C. R. N.; Chiavacci, L. A.; Pulcinelli, S. H.; Briois, V.; Santilli, C. V. *J Sol-Gel Sci Technol* **2014**, *70*, 317–328.
37. Mya, K. Y.; Pramoda, K. P.; He, C. B. *Polymer* **2006**, *47*, 5035–5043.
38. Chaker, J. A.; Santilli, C. V.; Pulcinelli, S. H.; Dahmouche, K.; Briois, V.; Judeinstein, P. *J. Mater. Chem.* **2007**, *17*, 744–757.
39. Moura, A. L. A.; Oliveira, L. K.; Ciuffi, K. J.; Molina, E. F. *J. Mater. Chem. A* **2015**, *3*, 16020–16032.
40. Santilli, C. V.; Chiavacci, L. A.; Lopes, L.; Pulcinelli, S. H.; Oliveira, A. G. *Chem. Mater.* **2009**, *21*, 463–467.
41. Caravieri, B. B.; de Jesus, N. A. M.; Oliveira, L. K.; Araujo, M. D.; Andrade, G. P.; Molina, E. F. *ACS Appl. Bio Mater.* **2019**, *2*, 1875–1883.
42. Korsmeyer, R. W.; Gurny, R.; Doelker, E.; Buri, P.; Peppas, N. A. *Int. J. Pharm.* **1983**, *15*, 25–35.

Figure Legends

Scheme 1. Synthetic procedure of the polyurea gel and corresponding network with hard (isocyanurate ring) and soft (polyether) domains.

Figure 1. FTIR spectra of the unloaded (black line) and loaded with Nap (red line), 5FU (blue line) and Nap+5FU (green line) PUr in the region between (a) 3000 – 700 cm^{-1} , (b) 1750 - 1300 cm^{-1} , and (c) 1300 – 700 cm^{-1} .

Figure 2: Photographs of the polyurea gel with versatile shaping showing perspective as (a) contact lenses, (b) film forming material for transdermal patch, (c) bulk material as LED devices and (d) packing application.

Figure 3. (a) SAXS curves for the unloaded PUr and containing Nap and 5Fu, separately and simultaneously; (b) representation of the correlation distance between the hard domains and soft domains in the polyurea network.

Figure 4. Contact angle measurements, as a function of time, for the unloaded polyurea organogel. Inset: Contact angle images of the PUr at different times.

Figure 5. Swelling capacities as a function of time for the unloaded polyurea and containing Nap and 5FU drugs, separately and simultaneously

Figure 6. DSC thermograms of the unloaded (black line) and loaded with Nap (red line), 5FU (blue line) and Nap+5FU (green line) PUr.

Figure 7. Time evolution of the UV–vis spectra collected during release experiments for (a) Nap, (c) 5FU and (e) Nap+5FU. Temporal evolution of cumulative profiles for (b) Nap, (d) 5FU and (f) Nap+5FU.

Figure 8. Plots of $\log (M_t/M_\infty)$ against $\log t$ for release experiments of (a) Nap, (b) 5FU and (c) Nap+5FU using water as aqueous medium.

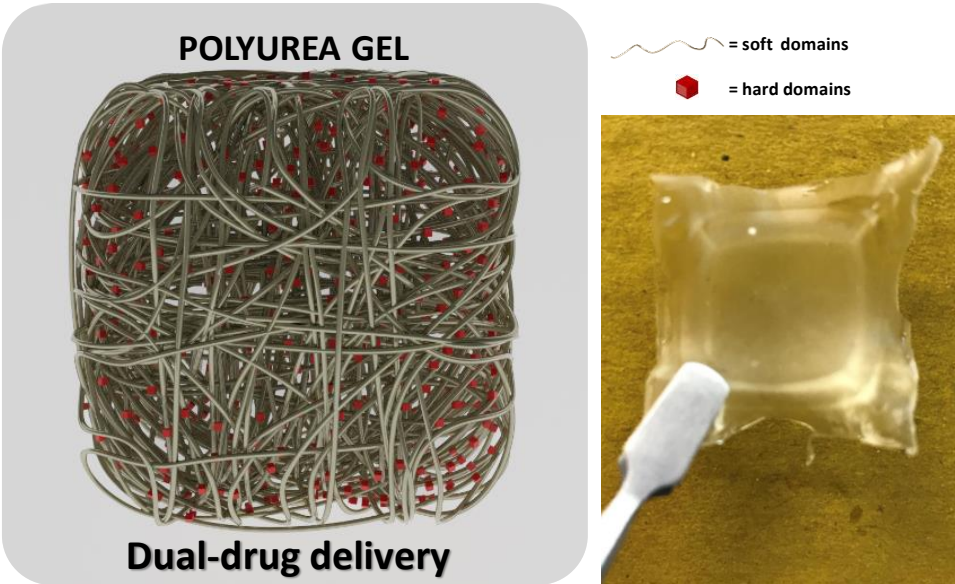
TABLE

Table 1. Thermal characteristics determined by DSC measurements of the unloaded and loaded PUr containing Nap, 5FU and both drugs simultaneously.

<i>Sample</i>	<i>T_g</i> (°C)	<i>T_m</i> (°C)	<i>D_c</i> (%)
PUr	-59	28	30
PUr-Nap	-58	31	27
PUr-5FU	-54	34	28
PUr-Nap-5FU	-56	32	27

Graphical Abstract

This class of polyurea gel containing two distinct drugs open up perspectives to prepare multifunctional materials for health, optical, and environmental applications



Supporting Information

Design of polyurea gel as versatile matrix bringing capabilities to carrier separately and simultaneously anticancer and anti-inflammatory drugs for delivery purposes

*Mariane A. de Resende,¹ Gabriele A. Pedroza,¹ Lucia H. G. M. C. Macêdo,¹ Ricardo de Oliveira,¹ Maria Amela-Cortes,² Yann Molard,² Eduardo F. Molina^{*1}*

¹*Universidade de Franca, Av. Dr. Armando Salles Oliveira 201, 14404-600 Franca, SP, Brazil*

²*Université Rennes, CNRS, ISCR - UMR 6226, ScanMAT – UMS 2001, F-35000 Rennes, France*

Corresponding author: Eduardo F. Molina

*email: eduardo.molina@unifran.edu.br

ORCID : 0000-0002-3574-2923

Naproxen and 5-FU analytical curves

The maximum absorbance values at 265 nm and 229 nm were used to construct the analytical curves of 5-FU and Nap drugs, respectively (Figure S1a and S1b).

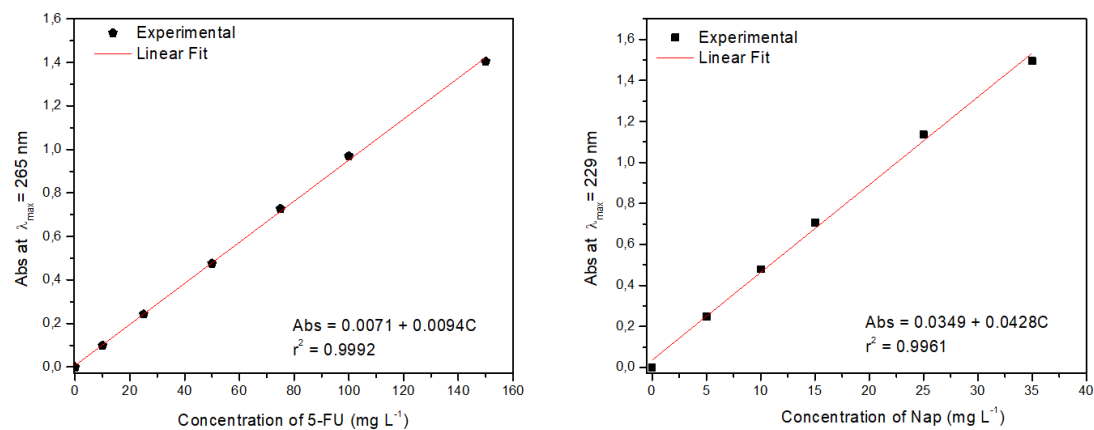


Figure S1. Analytical curve of (a) 5-FU and (b) Nap drug using distilled water (pH 6) as aqueous medium.

Polyurea macroscopic images

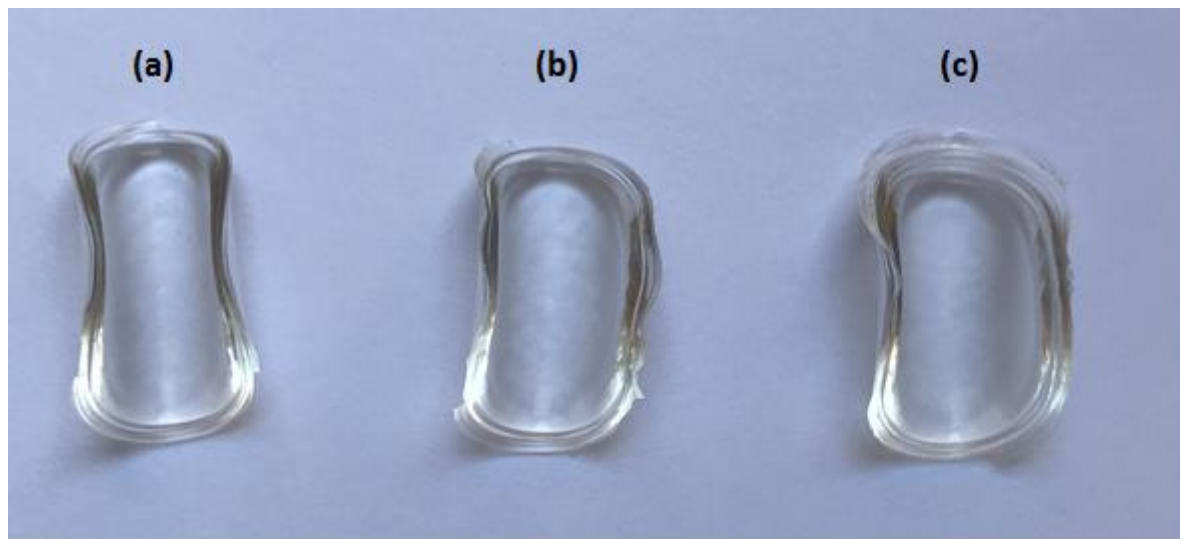


FIGURE S2: Photographs of the transparent and rubber polyurea gels (a) unloaded and loaded with (b) Naproxen and (c) 5-fluorouracil.

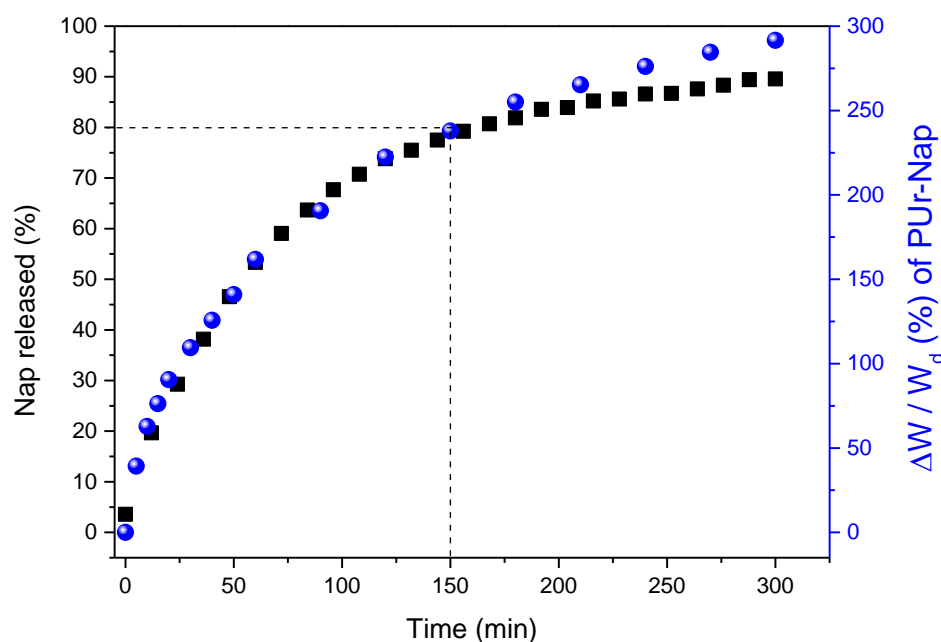


FIGURE S3: comparison between release profile and water uptake of PUR-Nap during the first 300 min of assays.

Korsmeyer–Peppas¹ kinetic model was applied to the drug release curves. Korsmeyer–Peppas model assumes a power law dependence to describe diffusion-controlled (Fickian) and swelling-controlled (Case II transport) mechanisms:

$$\frac{M_t}{M_\infty} = k t^n \quad \text{or} \quad \log \frac{M_t}{M_\infty} = \log k + n \log t$$

where M_t is the drug mass released at time t , M_∞ is the drug mass at $t = 0$, M_t/M_∞ is a fraction of the drug released at time t , k is the released rate constant and n is the released exponent which gives information regarding the drug transport mechanism. $n = 1$ characterized Case II transport indicate zero-order drug release, values of $n = 0.5$ indicate Fickian diffusion and n values between 0.50 and 0.90 can be regarded as an indication of the existence of both phenomena (anomalous transport).

Table S1. Amount released of Nap and 5FU at different times, Korsmeyer-Peppas parameters, and release mechanism of the drugs from PUr samples.

Sample	Amount released(%)		Korsmeyer-Peppas parameters ¹		Release mechanism
	at 150min	at final assay	n	R^2	
PUr-Nap	80	99	0.62	0.99	anomalous transport
PUr-5FU	60	72	0.62	0.99	anomalous transport
PUr-Nap*	60	100	0.70	0.99	anomalous transport
PUr-5FU*	40	77	0.68	0.99	anomalous transport

*sample containing both Nap and 5FU drugs (simultaneous release assay)

References

1. Korsmeyer, R. W.; Gurny, R.; Doelker, E.; Buri, P.; Peppas, N. A. Mechanisms of solute release from porous hydrophilic polymers. *Int. J. Pharm.* 1983, **15**, 25–35.